Analysis of Design Tradeoffs for Passively Damped Structural Joints

Jacky Prucz*
West Virginia University, Morgantown, West Virginia

An innovative means to enhance the inherent damping in structures is provided by the designed-in incorporation of viscoelastic materials in joints. The joints, as envisioned, are double-lap shear joints that dissipate energy when worked in an axial direction. To better understand the relationship between structural stiffness and structural damping as a function of important physical parameters, a one-dimensional analysis of a typical joint was developed. A quasistatic analytical model based on the complex modulus description of viscoelastic behavior is utilized. Potential applications to parametric studies, preliminary design, and experimental data analysis are illustrated. The predictions correlate well with expected physical behavior, simplified approximate models, and available test data.

Nomenclature

A,B = shear-stress coefficient, Eq. (1)
A_1,A_2 = real and imaginary parts of A, respectively
A_i,A_o = cross-sectional area of inner and outer adherends, respectively
A_s = cross-sectional area of elastic link
A_v = shear area of viscoelastic layer
B_1,B_2 = real and imaginary parts of B, respectively
b = width dimension of all joint components
C_β = parameter, defined in Eq. (26)
D = dissipated energy per unit volume per cycle
D_v = total dissipated energy per cycle
E_i,E_o = extensional modulus of inner and outer adherends, respectively
E_s = extensional modulus of elastic strip
G = complex shear modulus of viscoelastic material
G_1,G_2 = elastic and dissipative shear modulus, respectively
G_M = magnitude of complex shear modulus
l = overlap length
l_s = length of elastic link
H = nondimensional parameter, defined in Eq. (17)
i = $(-1)^{1/2}$
$I_1,\ldots,I_{12}$ = results of definite integrations, defined in the Appendix
K = nondimensional parameter, defined in Eq. (16)
K_j = axial stiffness of joint system
K_v = shear stiffness of adhesive layer
K_s = axial stiffness of elastic strip
K_r = reference axial stiffness
K_j' = relative joint stiffness with respect to K_r
P = amplitude of external load
S_d = specific damping capacity, defined in Eq. (27)
t_i,t_o = thickness of inner and outer adherends, respectively
t_s = thickness of elastic link
t_v = thickness of viscoelastic layer
$T_i(x),T_o(x)$ = internal force in inner and outer adherends, respectively
$T_s(x)$ = internal force in elastic link
$T_{og}(x)$ = internal force in the gap portion of outer adherend
$u_{og}(x)$ = axial displacement in gap portion of outer adherend
$u_i(x)$ = axial displacement in inner adherend
$u_{i1}(x),u_{i2}(x)$ = real and imaginary components, respectively, of $u_i(x)$
$u_s(x),u_o(x)$ = axial displacement in elastic link and outer adherend, respectively
U = total maximum strain energy per unit volume
U_t = total maximum strain energy stored in the joint
U_v,U_i,U_o,U_s,U_{og} = maximum strain energy per unit volume of viscoelastic material, inner adherend, outer adherend, elastic strip, and gap portion of outer adherend, respectively
$U_v',U_i',U_o',U_s',U_{og}'$ = strain energy contributions nondimensionalized with respect to U
U_{tv} = maximum strain energy per cycle in the viscoelastic material
V_v = volume of viscoelastic layers
W,W_r = weight of joint and reference weight, respectively
x = axial variable
β = complex parameter, defined in Eq. (2)
β_1,β_2 = real and imaginary parts of β, respectively
$\gamma(x)$ = shear-strain amplitude in adhesive layer
η = overall loss factor of joint system
η_v = loss factor of viscoelastic material
θ = loss angle, defined in Eq. (25)
$\tau(x)$ = shear-stress amplitude in adhesive layer
$\tau_1(x),\tau_2(x)$ = real and imaginary shear-stress components, respectively

Introduction

ALL structures must have sufficient inherent damping to keep vibration response, dynamic stress levels, noise, and fatigue within acceptable limits. Effective vibration and disturbance control is particularly critical to the achievement of precision spacecraft performance objectives. The tight orientation and deformation tolerances included in many future mission requirements for large space structures indicate that passive damping will be a key element in spacecraft vibration control.[1]

Presented as Paper 85-0780 at the AIAA/ASME/ASCE/AHS 26th Structures, Structural Dynamics and Materials Conference, Orlando, FL, April 15-17, 1985; received Aug. 12, 1985; revision received Jan. 28, 1986.

*Assistant Professor, Mechanical and Aerospace Engineering Department. Member AIAA.

High passive damping not only limits vibration amplitudes and shortens transient decay times, but also has favorable synergistic effects when combined with active controls. The performance of active modal control systems is enhanced significantly due to improved control system error tolerance, reduced levels of disturbances, and reduced control bandwidth requirements.[2]

The use of viscoelastic materials for the control of structural vibrations has been an approach used in an ever-increasing variety of applications as viscoelastic technology becomes well established and more widely known. The literature is replete with examples of constrained-layer viscoelastic damping treatments applied over large areas and viscous dampers applied to problem components.[3,4] While generally successful, some penalties are usually attendant because of the add-on approach typical of past applications. Damping treatments have been used as cures for unforeseen problems and, therefore, have been afterthoughts.

An innovative means to enhance the inherent damping in structures is provided by the designed-in incorporation of viscoelastic materials in joints. This combines the well-known damping capability of viscoelastic materials with the predominant influence of joints and supports on the overall damping of most structures.[5] The designed-in approach provides a promising opportunity to maximize the damping benefit, while minimizing the associated penalties in other structural properties. Preliminary theoretical and experimental research has been undertaken in the last two years for the development of generic, passively damped, joining concepts for space structures. New analytical models and experimental methods have been developed for the mechanical performance analysis of such joints and have been reported in Refs. 6–8.

In this paper, the development and application of a quasistatic analytical model for design analyses of passively damped joints based on a symmetric, double-lap configuration is presented. The primary objective is to provide an in-depth understanding of the structural interaction mechanism among the individual components of the joint and the associated effect upon the overall joint characteristics.

The double-lap configuration has been chosen because it is simple, widely used, and provides high shear deformation of the viscoelastic layers under axial loading of the members. The effect of a direct elastic connection between the members has also been included in the model. The elastic connection provides improved minimum stiffness and structural redundancy at elevated temperatures or in the case of viscoelastic materials with poor creep resistance. A typical joint specimen that has been designed and fabricated for the experimental investigation of this concept is shown in Fig. 1. Detailed information about the experimental program and results is given in Ref. 8.

Since the primary candidates for large space structures are repetitive lattice trusses,[9] the main loading direction considered in the design and testing of passively damped joint specimens is the axial one.

A fully elastic analytical model of a double-lap bonded joint with a restoring spring between the members has been developed independently and is presented in Refs. 6 and 7. The major contribution of the new, quasistatic model to the current state-of-the-art of bonded joints modeling, as it is reflected in Refs. 6, 7, 10, and 11, is the incorporation of viscoelastic behavior and the associated energy dissipation, which is necessary for a reliable assessment of the damping properties. Therefore, the model constitutes an essential step toward the implementation of the designed-in approach to damping enhancement of space structures.

Modeling Assumptions

Since the model is expected to be a practical tool for expedient design studies, the underlying guidelines for its development are simplicity and a reliable description of the actual physical behavior. The physical model shown in Fig. 2 is utilized to represent the actual joint configuration depicted in Fig. 1. Due to symmetry, only one-half of the joint needs to be considered for analysis, with no displacements allowed across the plane of symmetry. The terminology commonly used for conventional double-lap bonded joints is adopted here, as shown in Fig. 2.

The only external load acting on the joint is assumed to be a fluctuating axial force applied on one member, which is transferred through the joint to the other member. The analysis is conducted on a one-dimensional or planar basis which applies to plane stress or plane strain conditions. This simple context permits the evaluation of damping and stiffness properties associated with the primary, axial loading direction. The viscoelastic layers undergo pure shear deformation with constant shear stress across their thickness, whereas all of the others elements of the joint are subject to pure extensional deformation.

The inner and outer adherends of the joint and the elastic restoring element are assumed to display perfectly elastic behavior. The only source of damping in the joint is provided by the viscoelastic adhesive layers. The widely used complex modulus approach[12,13] is adopted here for the modeling of viscoelastic behavior. This implies the assumption of linear viscoelastic behavior in which the material behaves similar to a Voigt solid at any one frequency, so that its constitutive relations are similar to Hooke's law, but include complex rather than real material constants. The numerical values of the mechanical properties may change with the loading frequency, but the form of the constitutive relations remains unchanged at all frequencies.

The model is confined to a quasistatic analysis of the joint behavior under the fluctuating axial load, as is usually done in

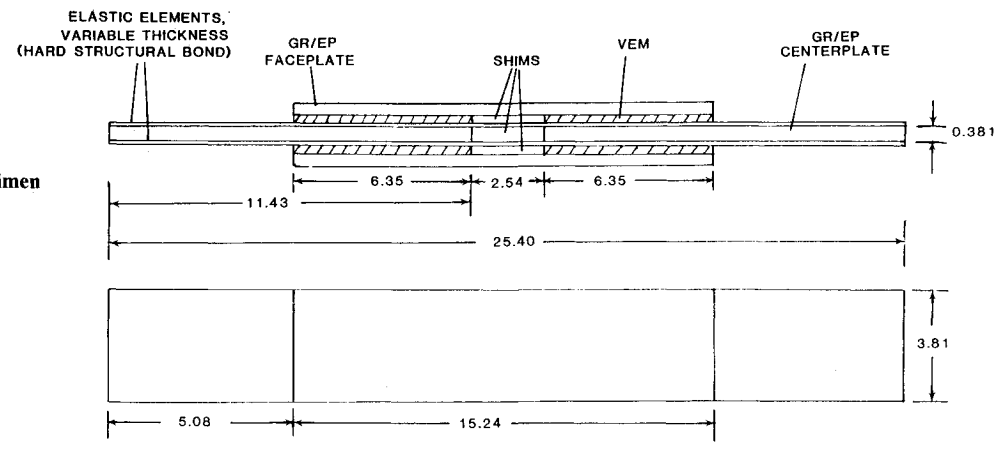

Fig. 1 Passively damped joint specimen with elastic elements.

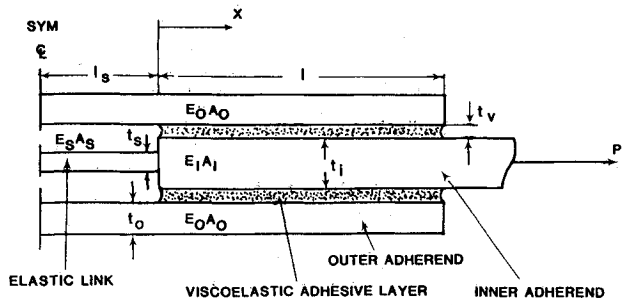

Fig. 2 Physical model of passively damped joint.

effectiveness investigations of constrained-layer damping treatments.[14] The quasistatic analysis is particularly well suited to space structures where low vibration frequencies are expected to be dominant[2] so that inertia effects may be neglected without serious errors, however, the dissipated energy has to be determined for a reliable estimation of damping.

Basic Equations

The structural part of the model relies upon the commonly used Hart-Smith analysis of double-lap bonded joints.[10] The model is modified to include the effect of a direct elastic connection between the inner adherends and the viscoelastic behavior of the adhesive material.

Stress equilibrium and kinematic conditions yield the shear stress distribution in the adhesive layers, following a development similar to that described in Ref. 10

$$\tau(x) = A\sinh(\beta x/l) + B\cosh(\beta x/l) \tag{1}$$

where the nondimensional parameter β is defined as

$$\beta^2 = \frac{G}{E_i}\left(\frac{E_i t_i}{E_o t_o} + 2\right)\frac{l^2}{t_v t_i} \tag{2}$$

Reference 15 includes a detailed description of this derivation. The constraints A and B are determined, as in the Hart-Smith model, from the boundary conditions imposed on the shear stress gradient at the ends of the overlap portion of the joint.

$$A = \frac{l}{\beta t_v} G\left(\frac{T_i(0)}{E_i t_i b} - \frac{T_o(0)}{E_o t_o b}\right) \tag{3}$$

$$B = \frac{l}{\beta t_v \sinh(\beta)} G\left[\frac{P - T_i(0)\cosh(\beta)}{E_i t_i b} + \frac{T_o(0)\cosh(\beta)}{E_o t_o b}\right] \tag{4}$$

In the absence of the direct elastic link between the inner adherends, which is the case in the Hart-Smith model, the inner adherend force must vanish at the boundary $x=0$, i.e., $T_i(0)=0$, so that only $T_o(0)$ remains to be evaluated. This is readily done by using the overall axial equilibrium condition of the joint, which in the general case may be expressed as follows:

$$T_i(0) + 2T_o(0) = P \tag{5}$$

In the present model, however, the inner adherends are interconnected through an elastic strip, so that $T_i(0) \neq 0$, and Eq. (5) is not sufficient. Further analysis is needed to derive an additional relationship between the four unknowns A, B, $T_i(0)$, and $T_o(0)$.

The internal axial force and displacement fields in the inner adherend and the overlap portion of the outer adherend vary in the x direction because of the interaction with the adhesive layers. The complete force and displacement distributions are determined from the adhesive stress distribution, Eq. (1), by integrations with respect to x of the corresponding equilibrium and constitutive equations. The elastic strip and the "gap" portion of the outer adherend, bounded by $x=-l_s$ and $x=0$, do not come in contact with the viscoelastic layers so that their internal forces and displacements are constant. The boundary conditions

$$u_s(-l_s) = 0, \qquad u_{og}(-l_s) = 0 \tag{6}$$

$$T_i(l) = P, \qquad T_o(l) = 0 \tag{7}$$

and the equilibrium and continuity conditions across the $x=0$ interfaces

$$T_{og}(0) = T_o(0), \qquad T_s(0) = T_i(0) \tag{8}$$

$$u_{og}(0) = u_o(0), \qquad u_s(0) = u_i(0) \tag{9}$$

enable the evaluation of all of the integration constants involved in the analysis. Substitution of the corresponding stress and displacement values into the constitutive relation of the adhesive layers.

$$\tau(0) = \frac{G}{t_v}[u_i(0) - u_o(0)] \tag{10}$$

yields the fourth relationship among the unknowns A, B, $T_i(0)$, and $T_o(0)$.

$$B = G\frac{l_s}{t_s}\left[\frac{T_i(0)}{E_s t_s b} - \frac{T_o(0)}{E_o t_o b}\right] \tag{11}$$

In the absence of the elastic restoring strip, both $T_i(0)$ and E_s are zero.

The four unknowns can be uniquely determined from the system of equations (3-5) and (11).

$$A = \frac{l}{\beta t_v}\frac{G}{E_i}\frac{P}{t_i b}\left[1 - \frac{K}{H}\left(2 + \frac{E_i t_i}{E_o t_o}\right)\right] \tag{12}$$

$$B = \frac{l_s}{t_v}\frac{G}{E_s}\frac{P}{t_s b}\left[1 - \frac{K}{H}\left(2 + \frac{E_s t_s}{E_o t_o}\right)\right] \tag{13}$$

$$T_i(0) = P[1 - 2(K/H)] \tag{14}$$

$$T_o(0) = P(K/H) \tag{15}$$

The nondimensional parameters K and H are defined as follows:

$$K = 1 - \frac{1 - \cosh(\beta)}{\beta\sinh(\beta)}\frac{l}{l_s}\frac{E_s t_s}{E_i t_i} \tag{16}$$

$$H = 2 + \frac{E_s t_s}{E_o t_o} + \frac{\cosh(\beta)}{\beta\sinh(\beta)}\frac{l}{l_s}\frac{E_s t_s}{E_i t_i}\left(2 + \frac{E_i t_i}{E_o t_o}\right) \tag{17}$$

These expressions yield dimensions of stress for A and B and dimensions of force for $T_i(0)$ and $T_o(0)$. In the limit $E_s t_s \to 0$, the values of $K \to 1$, and $H \to 2$, so that $T_i(0)$ tends to vanish, as it should without the restoring elastic strip between the inner adherends.

Damping Evaluation

The viscoelastic behavior of the adhesive layers is described by means of the complex modulus approach, i.e.,

$$G = G_1(1 + i\eta_v) \tag{18}$$

where the viscoelastic material loss factor is defined as

$$\eta_v = G_2/G_1 \tag{19}$$

The use of quasistatic and complex modulus modeling implies slow oscillatory external loading. The parameters describing the associated physical response of the joint are time-dependent, but inertia effects are ignored.

Since the shear modulus G of the adhesive layers is a complex quantity, as shown in Eq. (18), all of the other model parameters dependent on G, either explicitly or implicitly, are also complex quantities. The analysis required for the separation of the real and imaginary components from each other is described in Ref. 15. The final result is the separation between the storage and dissipative components of the shear-stress field in the viscoelastic layers:

$$\tau(x) = \tau_1(x) + i\tau_2(x) \tag{20}$$

where

$$\tau_1(x) = A_1 \cos\left(\frac{x}{l}\beta_2\right)\sinh\left(\frac{x}{l}\beta_1\right) - A_2 \sin\left(\frac{x}{l}\beta_2\right)\cosh\left(\frac{x}{l}\beta_1\right) + B_1 \cos\left(\frac{x}{l}\beta_2\right)\cosh\left(\frac{x}{l}\beta_1\right) - B_2 \sin\left(\frac{x}{l}\beta_2\right)\sinh\left(\frac{x}{l}\beta_1\right) \tag{21}$$

$$\tau_2(x) = A_2 \cos\left(\frac{x}{l}\beta_2\right)\sinh\left(\frac{x}{l}\beta_1\right) + A_1 \sin\left(\frac{x}{l}\beta_2\right)\cosh\left(\frac{x}{l}\beta_1\right) + B_2\cos\left(\frac{x}{l}\beta_2\right)\cosh\left(\frac{x}{l}\beta_1\right) + B_1 \sin\left(\frac{x}{l}\beta_2\right)\sinh\left(\frac{x}{l}\beta_1\right) \tag{22}$$

All of the parameters in Eqs. (21) and (22) represent real quantities, and are defined in the Nomenclature. The real and imaginary parts of the parameter β are expressed as follows:

$$\beta_1 = C_\beta \cos(\theta/2) \tag{23}$$

$$\beta_2 = C_\beta \sin(\theta/2) \tag{24}$$

where

$$\theta = \tan^{-1}(\eta_v) \tag{25}$$

$$C_\beta = \left[\frac{G_1}{E_i}\left(2 + \frac{E_i t_i}{E_o t_o}\right)\frac{l^2}{t_v t_i}(1+\eta_v^2)^{1/2}\right]^{1/2} \tag{26}$$

The parameters A_1, A_2, B_1, and B_2 have dimensions of stress; their complete expressions are given in the Appendix.

Although damping properties can be measured in terms of numerous parameters that are usually associated with various experimental techniques,[12] the most direct and useful measure is the specific damping capacity. In a dissipative system, the specific damping capacity is determined by the ratio between the energy dissipated in a unit volume per deformation cycle and the maximum potential energy stored in a unit volume during that cycle. Since energy dissipation occurs only in the viscoelastic layers, whereas strain energy is stored in all of the elastic components of the joint, the specific damping capacity is defined here as

$$S_d = D/U \tag{27}$$

where U is the sum of individual, unit volume, strain energy contributions, rather than the total strain energy stored in a unit volume of joint.

$$U = U_v + U_i + U_o + U_s + U_{og} \tag{28}$$

This definition of U facilitates parametric studies on the geometrical characteristics of various joint elements.

All of the strain energy contributions needed for the evaluation of the damping characteristics of the joint can be determined from the corresponding stress fields. According to the physical interpretation of the complex modulus concept, only the real stress field components are used for the evaluation of elastic strain energies.

The maximum value of the total elastic strain energy stored per cycle in the viscolatic layers is determined from the expression

$$U_{tv} = \frac{bt_v}{G_1}\int_0^l \tau_1^2(x)\,dx \tag{29}$$

An explicit final expression of U_{tv} in terms of known quantities can be developed by substituting the real shear-stress distribution from Eq. (21) into Eq. (29) and carrying out the integrations with respect to the axial variable, x.

The corresponding expression for U_v is

$$U_v = \frac{1}{2G_1}\left[A_1^2 I_8 + A_2^2 I_7 + B_1^2 I_6 + B_2^2 I_5 - \frac{I_1'}{2}(A_1A_2 + B_1B_2) + A_1B_1 I_{10} + A_2B_2 I_9 - A_2B_1 I_{11} - A_1B_2 I_{12}\right] \tag{30}$$

The symbols denoted by the letter I with various subscripts represent nondimensional quantities resulting from definite integrations of products between trigonometric and hyperbolic functions of real variables. Their complete expressions are given in the Appendix. Explicit expressions for the maximum strain energies stored during a cycle in each of the elastic components of the joint can be similarly developed, as described in detail in Ref. 15.

The total mechanical energy dissipated per cycle by the two viscoelastic layers can be evaluated by using the following equation[14]:

$$D_v = \int_{V_v} \pi G_2 |\gamma|^2 dV_v \tag{31}$$

The magnitude of the complex shear strain corresponding to the stress field defined by Eqs. (20–22) is substituted into Eq. (31) and, considering the one-dimensionality assumption of the model, the following equation is obtained for D_v:

$$D_v = \frac{\pi\eta_v bt_v}{G_1(1+\eta_v^2)}\int_0^l [\tau_1^2(x) + \tau_2^2(x)]\,dx \tag{32}$$

The corresponding final expression of the energy dissipated per unit volume of viscoelastic material per cycle is obtained after carrying out the integrations in Eq. (32).

$$D = \frac{\pi\eta_v}{2G_1(1+\eta_v^2)}[(A_1^2 + A_2^2)(I_7 + I_8) + (B_1^2 + B_2^2)(I_5 + I_6) + (A_1B_1 + A_2B_2)(I_9 + I_{10}) + (A_1B_2 - A_2B_1)(I_{11} - I_{12})] \tag{33}$$

The specific damping capacity of the joint can be calculated directly by substituting the appropriate energy expressions into Eq. (27).

An alternative way to decribe the damping performance of the joint is in terms of the commonly used concept of loss factor. However, an overall loss factor of the joint system needs to be defined for this purpose, and has to be clearly distinguished from the material loss factor of the viscoelastic layers, which is defined in Eq. (19). The system loss factor includes the effect of structural interactions between the various elements of the joint in addition to the effect of their in-

dividual mechanical properties. According to the general definition of loss factor in terms of energy quantities,[12,14] the system loss factor of a passively damped joint can be calculated by using the formula

$$\eta = \frac{D}{2\pi U} \tag{34}$$

Stiffness Evaluation

The foregoing development shows that the loss factor calculation of the whole joint system requires the evaluation of the total maximum strain energy stored during one cycle in all of the components of the joint. This strain energy can be used subsequently to evaluate the joint axial stiffness, according to the equation

$$K_j = \frac{P^2}{2U_t} \tag{35}$$

The basic definition of the stiffness concept provides an alternative method for its evaluation:

$$K_j = \frac{P}{u_i(l)} \tag{36}$$

The complete axial displacement distribution in the inner adherend is determined during the development of the model basic equations, so that it can be readily used for the axial stiffness evaluation in Eq. (36).

Results and Discussion

A computer program has been written for the analytical model developed above, and an extensive parametric and correlation study has been conducted. Selected numerical results are presented and discussed in order to illustrate the application of the model and compare its predictions with other theoretical and experimental data. The analysis of these results provides an in-depth understanding of the operating structural interactions among the various components of a passively damped joint.

Correlation Studies

Numerical results generated by a fully elastic model of a double-lap bonded joint with a restoring spring between the inner adherends are given in Ref. 7. Figure 3 illustrates the good correlation that exists between the predictions of the fully elastic and viscoelastic models.

The following constant numerical parameters have been selected for Fig. 3:

$P = 1$ lb (4.45 N)

$E_i, E_o = 8.5 \times 10^6$ psi (58,624 MPa)

$t_i = 0.2$ in. (0.508 cm)

$t_o = 0.1$ in. (0.254 cm)

$t_s = 0.047$ in. (0.119 cm)

$b = 1.0$ in. (2.54 cm)

$l_s = 0.5$ in. (1.27 cm)

The correlation is based on the two parameters used in Ref. 7, namely the total strain energy stored in the adhesive layers, U_{tv}, and the elastic displacement at the external end of the inner adherend, $u_{i1}(l)$.

Figure 3 shows the effect of the overlap length on these two parameters for a soft elastic link. It displays also the end deflection results associated with the simple design equation

$$K_v = G_M A_v / t_v \tag{37}$$

which yields the equivalent shear stiffness of an adhesive layer assuming uniform shear stress distribution over the whole area, A_v, and no elastic link between the inner adherends. As mentioned in Refs. 7 and 8, Eq. (37) has been used for the design of passively damped joint test specimens.

All of the three methods compared in Fig. 3 predict the same physical behavior associated with the increase of the overlap length. The two analytical models agree extremely well in the perfectly elastic case shown in Fig. 3, despite minor differences in their mathematical formulation (see Ref. 15). The approximate equation (37) generates higher deflection values than the more accurate analytical models. This is because it assumes that all of the strain energy of the joint is stored in the adhesive layers. Therefore, it yields lower predictions for the overall joint stiffness than the actual values.

An important application of the quasistatic analytical model is the prediction of overall stiffness and damping properties of a joint when the properties of its constituents are known. Figures 4 and 5 illustrate, respectively, how the joint axial stiffness and loss factor can be evaluated as a function of the elastic shear modulus and loss factor of the viscoelastic

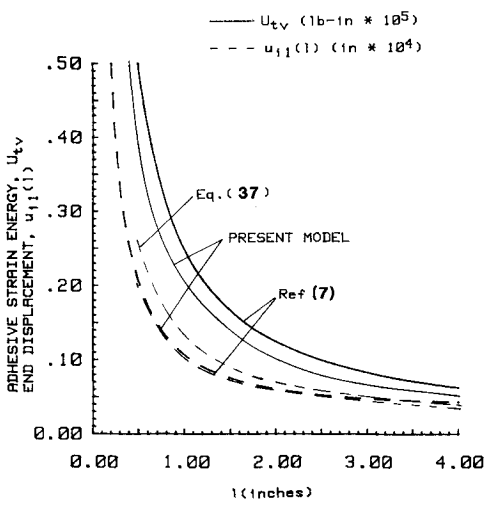

Fig. 3 Correlation of overlap length effect for $K_s = 20$ lb/in., $G_1 = 1000$ psi, $\eta_v = 0$, $t_v = 0.02$ in.

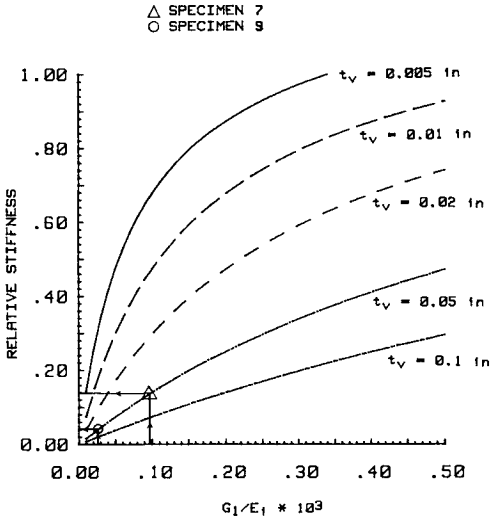

Fig. 4 Stiffness test data correlation for $K_s = 20$ lb/in., $l = 3.0$ in., $\eta_v = 0$, $K_r = 1{,}755{,}000$ lb/in.

material used in the joint. The constant parameters used in these figures are

$P = 1$ lb (4.45 N)

$E_i, E_o = 15.6 \times 10^6$ psi (107,593 MPa)

$t_i, t_o = 0.15$ in. (0.38 cm)

$t_s = 0.047$ in. (0.12 cm)

$l = 3.0$ in. (7.62 cm)

$l_s = 0.5$ in. (1.27 cm)

$b = 1.5$ in. (3.81 cm)

The primary difference between the test specimens selected for this illustration is the type of adhesive material. The adhesive thickness is about 0.05 in. for all of these specimens and none includes an elastic, return-to-zero element in its configuration. Material data available, according to Ref. 7, for the particular adhesives used in these joints are utilized in Figs. 4 and 5 for the prediction of the overall stiffness and damping characteristics, respectively.

The viscoelastic material data and the corresponding joint properties predicted by the quasistatic model are given in Table 1. Experimental data measured on the same joint specimens by the hysteresis-loop technique are also included in Table 1.

A complete description of the test specimens, procedures, and results is given in Refs. 8 and 15. Both the joint test data and the reference material data have been measured at room temperature and at very low frequencies (about 0.1 Hz and below) which are close to each other but not exactly equal.[7,8] The results in Table 1 show good agreement between the predicted joint characteristics and the experimental data.

Parametric Analysis

The quasistatic model enables expedient preliminary sizing and materials selection for passively damped joints of the double-lap configuration to satisfy overall design requirements.

Tradeoff analyses between the damping benefit and the stiffness and weight penalties can be effectively conducted with this model.

Figures 6-8 illustrate examples of parametric studies for the selection of mechanical properties of the individual joint components. The numerical parameters selected for this illustration correspond to representative test specimens.[8]

The constant parameters used in Figs. 6-8 are:

$P = 1$ lb (4.45 N)

$E_i, E_o = 15.6 \times 10^6$ psi (107,593 MPa)

$t_i = 0.15$ in. (0.38 cm)

$t_o = 0.15$ in. (0.38 cm)

$t_s = 0.047$ in. (0.12 cm)

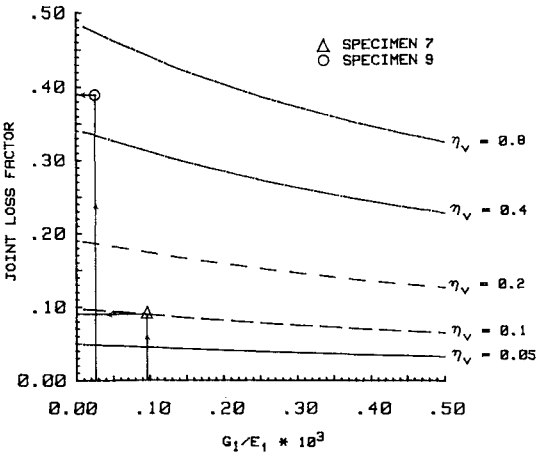

Fig. 5 Damping test data correlation for $K_s = 20$ lb/in., $t_v = 0.05$, $l = 3.0$ in.

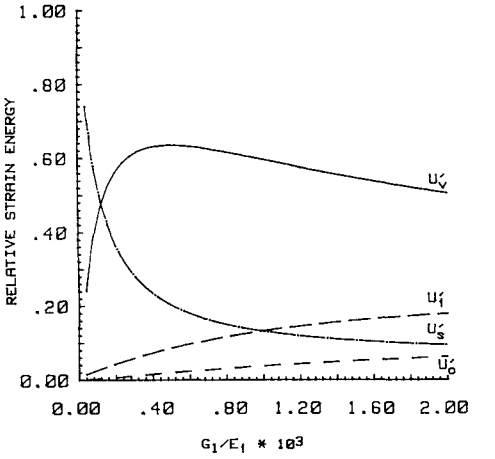

Fig. 6 Effect of adhesive stiffness on strain energy distribution for $K_s = 200{,}000$ lb/in., $l = 2.0$ in., $t_v = 0.02$ in., $\eta_v = 0.3$.

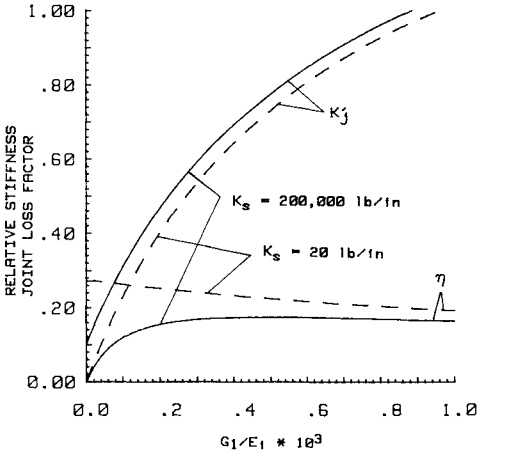

Fig. 7 Performance dependence on adhesive stiffness for $\eta_v = 0.3$, $K_r = 1{,}755{,}000$ lb/in.

Table 1 Prediction of joint properties from material data

Specimen no.	Viscoelastic material	Available material data[a]			Joint stiffness, lb/in.		Joint loss factor	
		Source	G_1, psi	η_v	Predicted	Measured	Predicted	Measured
5	DYAD 606	UDRI[b]	143	0.53	26,325	28,688	0.385	0.47
7	EA 9326		1,500	0.1-0.3	236,925	191,102	0.09	0.11
9	SMRD 100 F90	GE	399	0.57	70,200	77,908	0.39	0.31

[a]Based on information given in Ref. 7. [b]University of Dayton Research Institute.

$t_v = 0.02$ in. (0.05 cm)

$l = 2.0$ in. (5.08 cm)

$l_s = 0.5$ in. (1.27 cm)

$b = 1.5$ in. (3.81 cm)

Figure 6 shows the strain energy distribution among the different elements of the joint for a stiff elastic strip. Since the adhesive layers are the softest element of the joint, they usually share most of its strain energy. In the case of a stiff elastic strip, no significant shear deformation occurs in the adhesive layers for very low values of G_1, so that the dominant contribution to the total strain energy of the joint comes from the elastic link. The strain energy share of the adhesive starts to increase as G_1 increases to a certain optimum values, i.e., about 6000 psi (41.38 MPa) in Fig. 6, afer which it decreases as the adhesive becomes even stiffer.

The direct consequences of the strain energy distributions discussed above on the two major performance parmeters of the joint, namely, damping and stiffness, are illustrated in Fig. 7. The reference stiffness used to nondimensionalize the stiffness parameter is that of a homogeneous 2.0-in. (5.08 cm)-long bar (as the chosen overlap length) composed of the same material as the adherend and having the same cross section. Since the adhesive material loss factor is assumed to be constant in Fig. 7, the total loss factor of the joint system is determined by the amount of shear deformation induced in the adhesive layers. Consequently, it displays the same type of behavior as the adhesive strain energy curve in Fig. 6.

The total axial stiffness of the joint is significantly enhanced for both soft and stiff elastic connection elements by selecting stiffer adhesive materials. The use of stiff viscoelastic materials, with elastic shear moduli in the range 9000-15,000 psi (62-103 MPa), yields better damping-stiffness tradeoffs since the stiffness enhancement achievable by increasing G_1 is more pronounced than the associated reduction in the damping benefit.

This conclusion is further illustrated in Fig. 8 in connection with the effect of the adhesive material loss factor for a stiff elastic strip. The relative axial stiffness and the total loss factor of the joint are presented for three different stiffness levels of the viscoelastic material. Unlike the former figures, where η_v was constant and G_1 was chosen to represent the adhesive stiffness, in Fig. 8 the stiffness level of the adhesive material is represented by the magnitude of the shear complex modulus, G_M, since η_v is a variable.

$$G_M = G_1(1+\eta_v)^{1/2} \tag{38}$$

For each value of η_v, the values of G_1 and G_2 corresponding to the selected stiffness level, G_M, are calculated directly from Eqs. (19) and (38). When a stiff elastic strip is included in the joint (see for example, Fig. 8), the use of stiff viscoelastic materials is especially important, since both the stiffness performance and the damping benefit improve significantly as G_M becomes larger. This effect is obviously related to the strain energy share of the adhesive layers, as discussed previously in connection with Fig. 6.

The preceding discussion about the mechanical properties of the viscoelastic material raises the great importance of an appropriate matching between the stiffness levels of the adhesive and the elastic strip. Soft viscoelastic materials should be combined with soft elastic strips; however, when stiffer adhesive can be used, the elastic strip stiffness may also be increased.

The main geometrical parameters expected to affect the overall damping and stiffness of the joint are the shear area of the viscoelastic layers and their thickness.

The shear area effect is illustrated in Fig. 9. Since the width dimension is kept constant, e.g., $b = 1.5$ in. (3.81 cm), as in the former figures, the changes in shear area are obtained by varying the overlap length l. Longer overlaps are desirable, in general, from the tradeoff standpoint between the damping benefit and the stiffness penalty.

However, in addition to geometrical constraints, longer overlaps are associated with higher weight penalties. This effect is illustrated in Fig. 9, where the ratio between the actual weight of the joint and a constant reference weight is plotted

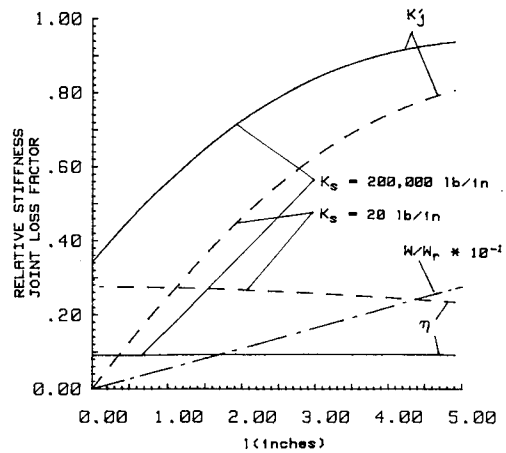

Fig. 9 Performance dependence on overlap length for $G_1 = 1000$ psi. $t_v = 0.02$ in., $\eta_v = 0.3$, $K_r = 585{,}000$ lb/in., $W_r = 0.0734$ lb.

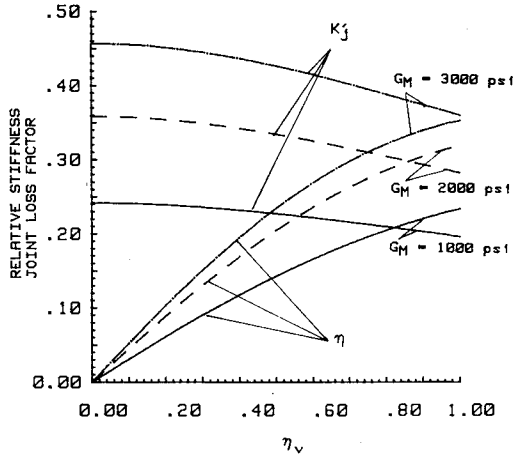

Fig. 8 Performance dependence on loss factor of adhesive material for $K_s = 200{,}000$ lb/in., $K_r = 1{,}755{,}000$ lb/in.

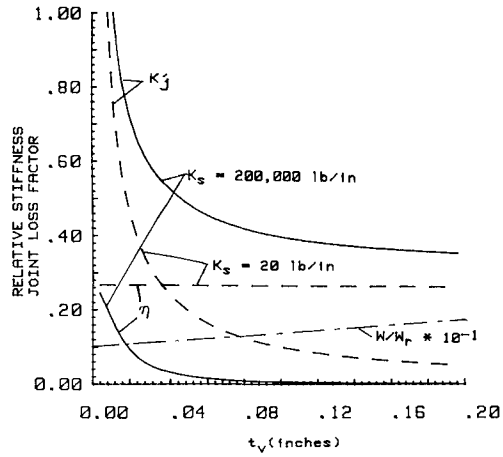

Fig. 10 Performance dependence on adhesive thickness for $G_1 = 1000$ psi, $l = 2.0$ in., $\eta_v = 0.3$, $K_r = 585{,}000$ lb/in., $W_r = 0.0734$ lb.

against the overlap length. A mass density of 0.0544 lb/in.^{3} (1.511 g/cm^3) is assumed for the adherends, whereas, the density of the viscoelastic material is chosen to be 0.04 lb/in.^{3} (1.11 g/cm^3). The reference weight is that of an ideal joint composed of the same adherend as the actual one, but with no adhesive layers and a fixed overlap length of 2.0 in. (5.08 cm).

Figure 10 displays the adhesive thickness effect on the overall performance of a passively damped joint. Thicker adhesive layers have lower shear stiffness and yield poorer stiffness performance of the joint. The total loss factor is not affected by the adhesive thickness in the case of a soft elastic link, but decreases asymptotically to zero as t_v increases in the case of a stiff elastic link since the adhesive layers become insignificant in the load transfer process through the joint. Therefore, the adhesive layers should be as thin as possible, especially when elastic elements are included in the joint. This is desirable also from the weight penalty standpoint, as shown in Fig. 10.

Conclusions

A quasistatic analytical model and illustrative examples of how the designed-in approach can be applied advantageously in the development of passively damped joints for space structures have been presented.

A dominant factor to be considered in the tradeoff analysis between the damping benefit and the stiffness penalty associated with the use of passively damped joints for space structures is the elastic shear modulus of the viscoelastic adhesive. Although stiff viscoelastic materials usually have lower loss factors than soft materials, they provide better damping-stiffness tradeoffs and seem to be preferable for application in passively damped joints. Proper design configurations may compensate against the use of relatively low-loss-factor materials by enhancing the contribution of the adhesive layers to the total strain energy of the joint. Stiff viscoelastic materials can be matched with stiff elastic, return-to-zero elements without an unacceptable drop in the overall damping performance of the joint.

This paper proves the tremendous importance of modeling and understanding structural interactions among the various components of passively damped joints. It presents a very useful analytical model that provides a quantitative relationship between the overall characteristics of such a joint and the corresponding properties of its individual constituents. The model is an expedient design tool suitable for tradeoff studies between the damping enhancement and the associated stiffness and weight penalties. It represents an essential step toward the implementation of the designed-in approach to passive damping enhancement.

Appendix

The real parameters A_1, A_2, B_1, B_2 in Eqs. (21) and (22) are defined as follows:

$$A_1 = \frac{l}{t_v}\frac{P}{t_i b}\frac{G_1}{E_i}\left[\frac{\beta_1+\eta_v\beta_2}{\beta_1^2+\beta_2^2} - \frac{K_{h1}(\beta_1+\eta_v\beta_2)+K_{h2}(\beta_2-\eta_v\beta_1)}{\beta_1^2+\beta_2^2}\left(2+\frac{E_i t_i}{E_o t_o}\right)\right] \quad \text{(A1)}$$

$$A_2 = \frac{l}{t_v}\frac{P}{t_i b}\frac{G_1}{E_i}\left[\frac{\eta_v\beta_1-\beta_2}{\beta_1^2+\beta_2^2} - \frac{K_{h1}(\eta_v\beta_1-\beta_2)+K_{h2}(\beta_1+\eta_v\beta_2)}{\beta_1^2+\beta_2^2}\left(2+\frac{E_i t_i}{E_o t_o}\right)\right] \quad \text{(A2)}$$

$$B_1 = \frac{l_s}{t_v}\frac{P}{t_s b}\frac{G_1}{E_s}\left[1-(K_{h1}-\eta_v K_{h2})\left(2+\frac{E_s t_s}{E_o t_o}\right)\right] \quad \text{(A3)}$$

$$B_2 = \frac{l_s}{t_v}\frac{P}{t_s b}\frac{G_1}{E_s}\left[\eta_v-(K_{h2}+\eta_v K_{h1})\left(2+\frac{E_s t_s}{E_o t_o}\right)\right] \quad \text{(A4)}$$

The nondimensional parameters K_{h1} and K_{h2} are given by

$$K_{h1} = \frac{K_1 H_1 + K_2 H_2}{H_1^2+H_2^2} \quad \text{(A5)}$$

$$K_{h2} = \frac{K_2 H_1 - K_1 H_2}{H_1^2+H_2^2} \quad \text{(A6)}$$

where

$$K_1 = 1 - \frac{B_{h1}-B_{h1}C_{h1}-B_{h2}C_{h2}}{B_{h1}^2+B_{h2}^2}\frac{l}{l_s}\frac{E_s t_s}{E_i t_i} \quad \text{(A7)}$$

$$K_2 = \frac{B_{h2}+B_{h1}C_{h2}-B_{h2}C_{h1}}{B_{h1}^2+B_{h2}^2}\frac{l}{l_s}\frac{E_s t_s}{E_i t_i} \quad \text{(A8)}$$

$$H_1 = 2+\frac{E_s t_s}{E_o t_o} + \frac{(B_{h1}C_{h1}+B_{h2}C_{h2})}{B_{h1}^2+B_{h2}^2}\frac{l}{l_s}\frac{E_s t_s}{E_i t_i}\left(2+\frac{E_i t_i}{E_o t_o}\right) \quad \text{(A9)}$$

$$H_2 = \frac{B_{h1}C_{h2}-B_{h2}C_{h1}}{B_{h1}^2+B_{h2}^2}\frac{l}{l_s}\frac{E_s t_s}{E_i t_i}\left(2+\frac{E_i t_i}{E_o t_o}\right) \quad \text{(A10)}$$

and

$$S_{h1} = \cos(\beta_2)\sinh(\beta_1) \quad \text{(A11)}$$

$$S_{h2} = \sin(\beta_2)\cosh(\beta_1) \quad \text{(A12)}$$

$$C_{h1} = \cos(\beta_2)\cosh(\beta_1) \quad \text{(A13)}$$

$$C_{h2} = \sin(\beta_2)\sinh(\beta_1) \quad \text{(A14)}$$

$$B_{h1} = \beta_1 S_{h1} - \beta_2 S_{h2} \quad \text{(A15)}$$

$$B_{h2} = \beta_2 S_{h1} + \beta_1 S_{h2} \quad \text{(A16)}$$

The complete expressions of the nondimensional parameters $I_1,\ldots,I_{12}$ included in Eqs. (30) and (33) are listed below:

$$I_1 = \frac{1}{\beta_1^2+\beta_2^2}(\beta_1 \sin\beta_2 \cosh\beta_1 - \beta_2 \cos\beta_2 \sinh\beta_1) \quad \text{(A17)}$$

$$I_2 = \frac{1}{\beta_1^2+\beta_2^2}(\beta_1 \cos\beta_2 \sinh\beta_1 + \beta_2 \sin\beta_2 \cosh\beta_1) \quad \text{(A18)}$$

$$I_1' = \frac{1}{2(\beta_1^2+\beta_2^2)}(\beta_1 \sin 2\beta_2 \cosh 2\beta_1 - \beta_2 \cos 2\beta_2 \sinh 2\beta_1) \quad \text{(A19)}$$

$$I_2' = \frac{1}{2(\beta_1^2+\beta_2^2)}(\beta_1 \cos 2\beta_2 \sinh 2\beta_1 + \beta_2 \sin 2\beta_2 \cosh 2\beta_1) \quad \text{(A20)}$$

$$I_3 = \frac{1}{\beta_1^2+\beta_2^2}(\beta_1 \cos\beta_2 \cosh\beta_1 + \beta_2 \sin\beta_2 \sinh\beta_1 - \beta_1) \quad \text{(A21)}$$

$$I_4 = \frac{1}{\beta_1^2+\beta_2^2}(\beta_1 \sin\beta_2 \sinh\beta_1 - \beta_2 \cos\beta_2 \cosh\beta_1 + \beta_2) \quad \text{(A22)}$$

$$I_5=\frac{1}{4}\left[\frac{\beta_2^2\ \sinh 2\beta_1}{2\beta_1(\beta_1^2+\beta_2^2)}-\left(1-\frac{\sin 2\beta_2}{2\beta_2}\right)\right.$$
$$\left.+\frac{\sin\beta_2}{\beta_1^2+\beta_2^2}(\beta_1\ \sin\beta_2\ \sinh 2\beta_1-\beta_2\cos\beta_2\ \cosh 2\beta_1)\right] \quad \text{(A23)}$$

$$I_6=\frac{1}{4}\left[\frac{\beta_2^2\ \sinh 2\beta_1}{2\beta_1(\beta_1^2+\beta_2^2)}+\left(1+\frac{\sin 2\beta_2}{2\beta_2}\right)\right.$$
$$\left.+\frac{\cos\beta_2}{\beta_1^2+\beta_2^2}(\beta_1\cos\beta_2\ \sinh 2\beta_1+\beta_2\ \sin\beta_2\ \cosh 2\beta_1)\right] \quad \text{(A24)}$$

$$I_7=\frac{1}{4}\left[\frac{\beta_2^2\ \sinh 2\beta_1}{2\beta_1(\beta_1^2+\beta_2^2)}+\left(1-\frac{\sin 2\beta_2}{2\beta_2}\right)\right.$$
$$\left.+\frac{\sin\beta_2}{\beta_1^2+\beta_2^2}(\beta_1\ \sin\beta_2\ \sinh 2\beta_1-\beta_2\cos\beta_2\ \cosh 2\beta_1)\right] \quad \text{(A25)}$$

$$I_8=\frac{1}{4}\left[\frac{\beta_2^2\ \sinh 2\beta_1}{2\beta_1(\beta_1^2+\beta_2^2)}-\left(1+\frac{\sin 2\beta_2}{2\beta_2}\right)\right.$$
$$\left.+\frac{\cos\beta_2}{\beta_1^2+\beta_2^2}(\beta_1\ \cos\beta_2\ \sinh 2\beta_1+\beta_2\ \sin\beta_2\ \cosh 2\beta_1)\right] \quad \text{(A26)}$$

$$I_9=\frac{1}{2(\beta_1^2+\beta_2^2)}\left[\frac{\beta_2^2(\cosh 2\beta_1-1)}{2\beta_1}\right.$$
$$\left.+\sin\beta_2(\beta_1\ \sin\beta_2\ \cosh 2\beta_1-\beta_2\ \cos\beta_2\ \sinh 2\beta_1)\right] \quad \text{(A27)}$$

$$I_{10}=\frac{1}{2(\beta_1^2+\beta_2^2)}\left[\frac{\beta_2^2(\cosh 2\beta_1-1)}{2\beta_1}\right.$$
$$\left.+\cos\beta_2(\beta_1\ \cos\beta_2\ \cosh 2\beta_1+\beta_2\ \sin\beta_2\ \sinh 2\beta_1)-\beta_1\right] \quad \text{(A28)}$$

$$I_{11}=\frac{1}{4}\left[\frac{\beta_2}{\beta_1^2+\beta_2^2}+\frac{1}{\beta_2}(1-\cos 2\beta_2)\right.$$
$$\left.+\frac{1}{\beta_1^2+\beta_2^2}(\beta_1\ \sin 2\beta_2\ \sinh 2\beta_1-\beta_2\ \cos 2\beta_2\ \cosh 2\beta_1)\right] \quad \text{(A29)}$$

$$I_{12}=\frac{1}{4}\left[\frac{\beta_2}{\beta_1^2+\beta_2^2}+\frac{1}{\beta_2}(\cos 2\beta_2)\right.$$
$$\left.+\frac{1}{\beta_1^2+\beta_2^2}(\beta_1\ \sin 2\beta_2\ \sinh 2\beta_1-\beta_2\ \cos 2\beta_2\ \cosh 2\beta_1)\right] \quad \text{(A30)}$$

Acknowledgments

This effort was performed at the Georgia Institute of Technology, and supported by the Air Force Office of Scientific Research under Contract F49620-83-C-0017.

References

[1]Amos, A.K. and Hallauer, W.L., ed., "Second Forum on Space Structures," sponsored by the Air Force Office of Scientific Research, Air Force Flight Dynamics Laboratory, NASA Langley Research Center, McLean, VA, June 1984.

[2]Trudell, R.W., Curley, R.C., and Rogers, L.C., "Passive Damping in Large Precision Space Structures," AIAA Paper 80-0677, *Proceedings of the AIAA/ASME/ASCE/AHS 21st Structures, Structural Dynamics and Materials Conference,* Seattle, WA, May 1980, pp. 124-136.

[3]Nakra, B.C., "Vibration Control with Viscoelastic Materials," *Shock and Vibration Digest,* Vol. 8, June 1975, pp. 3-12.

[4]Trapp, W.J. and Bowie, G.E., "Perspectives on Damping," *Damping Applications for Vibration Control,* edited by P.J. Torvik, ASME Winter Annual Meeting, Chicago, IL, 1980.

[5]Beards, C.F., "Damping in Structural Joints," *Shock and Vibration Digest,* Vol. 11, Sept. 1979, pp. 35-41.

[6]Trudell, R.W., Rehfield, L.W., Reddy, A.D., Prucz, J., and Peebles, J., "Passively Damped Joints for Advanced Space Structures," *Proceedings of the Vibration Damping Workshop,* Long Beach, CA, Feb. 1984, pp. DDD-1-DDD-29.

[7]Trudell, R.W. and Blevins, C.E., "Passively Damped Joints for Advanced Space Structures," McDonnell Douglas Astronautics Company, Huntington Beach, CA, Annual Tech. Rept. MDC H1178, June 1984.

[8]Prucz, J., Reddy, A.D., Rehfield, L.W., and Trudell, R.W., "Experimental Characterization of Passively Damped Joints for Space Structures," *Journal of Spacecraft and Rockets,* Vol. 23, Nov.-Dec. 1986, pp. 568-575.

[9]Noor, A.K., "Assessment of Current State of the Art in Modeling Techniques and Analysis Methods for Large Space Structures," *Modeling, Analysis and Optimization Issues for Large Space Structures,* NASA CP 2258, May 1982, pp. 5-32.

[10]Hart-Smith, L.J., "Adhesive-Bonded Double-Lap Joints," NASA CR-112235, Jan. 1973.

[11]Loss, K.R., and Kedward, K.T., "Modeling and Analysis of Peel and Shear Stresses in Adhesively Bonded Joints," AIAA Paper 84-0913, *Proceedings of the AIAA/ASME/ASCE/AHS 25th Structures, Structural Dynamics and Materials Conference,* Palm Springs, CA, May 1984, pp. 222-231.

[12]Bert, C.W., "Material Damping: An Introductory Review of Mathematical Models, Measures and Experimental Techniques," *Journal of Sound and Vibration,* Vol. 29, No. 2, 1973, pp. 129-153.

[13]Christensen, R.M., *Theory of Viscoelasticity, An Introduction,* Academic Press, New York, 1971.

[14]Torvik, P.J., "The Analysis and Design of Constrained Layer Damping Treatments," *Damping Applications for Vibration Control,* edited by P.J. Torvik, ASME Winter Annual Meeting, Chicago, IL, 1980, AMD-Vol. 38, pp 85-112.

[15]Prucz, J., "Analytical and Experimental Methodology for Evaluating Passively Damped Structural Joints," Ph.D. Dissertation, Georgia Institute of Technology, May 1985.